

Pd-C film for sensor applications

R. Belka², E. Czerwos¹, J. Kęczkowska², E. Kowalska¹, M. Kozłowski¹, J. Rymarczyk¹, M. Suchańska²

¹ Tele- & Radio Research Institute, 00-241 Warszawa, ul. Długa 44/50

² Kielce University of Technology, 25-413 Kielce, Al.1000-lecia P.P. 7

Corresponding author: r.belka@tu.kielce.pl

INTRODUCTION

Carbon nanostructures are known as very promising materials for hydrogen sensors and storage [1,2]. In literature one can find information about influence different type of doping on storage capacity [3]. Recently, carbonaceous-Pd films are considered as very perspective nanostructures for these applications due to palladium activity toward hydrogen [4].

We present results of characterization by SEM, AFM and Raman spectroscopy of films obtained in 2-steps method. These films are composed of nanoporous carbonaceous matrix and Pd nanocrystals. We found that the structure and topography of final films depend on the content of palladium initially introduced in first step do not depend on a substrate kind and its topography.

EXPERIMENTAL

SAMPLE PREPARATION

C-Pd films were obtained by 2-steps method on substrates with different topography. In the first step - PVD (Physical Vapor Deposition) method from two separated sources was used: one source contained fullerene C₆₀ and second contained palladium acetate Pd(C₂H₃O₂)₂. Depending on kind of substrates, temperature of sources, the rate of growth of nanostructures the film obtained by PVD was composed of a carbonaceous matrix and Pd grains placed in it. The concentration of Pd in the studied films is presented in Tab.1. Samples were studied with SEM, AFM and Raman spectroscopy.

The second step was CVD method. In this step PVD films were modified. Modification zones of CVD reactor are shown in Fig. 1 In the first zone maximum temperature was of 180° C. In zone II with temperature of 650° C decomposition of the solvent (xylene) and the conversion PVD film take place [5].

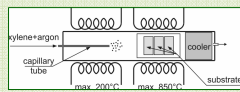


Fig.1. Schema of experimental CVD set-up

Table 1 List of the sample

Sample number	Substrates	Pd content [wt.%]
(1)	Hill-like surface	7.98
(2)	Flat surface	24
(3)	Flat surface	27.91

SEM and AFM study

Topography and morphology of films were studied with Scanning Electron Microscopy (SEM) and Atomic Force Microscopy (AFM). SEM investigations were performed with the JEOL 7600F field emission scanning electron microscope operating at 5 keV incident energy. AFM studies were carried out with EXPLORER 2000 (Thermomicroscopes) in non-contact mode with standard Si3N4 tip in the ambient atmosphere.

SEM images of PVD films with highest Pd content and on flat substrates are presented in Fig. 2. SEM images of these samples show that grain's sizes are different and distances between grains is also different. Grains size of the sample (2) is about 200nm (fig. 2A) and of the sample (3) above 500nm (fig.3).

SEM images of CVD films are presented in Fig. 3. After modification in CVD process PVD films become porous. Porosity depends on Pd content in PVD film. For sample (1) with lower Pd concentration film is more porous. From SEM images analysis (for secondary and back scattered electrons) we deduced that porous matrix is mostly carbonaceous while grains placed in this matrix are Pd nanocrystals.

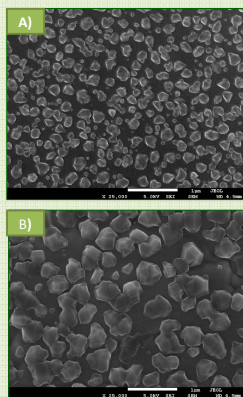


Fig.2. SEM images for samples obtained in PVD process on flat substrate: 24% wt. of Pd (A) and 27.9% wt. of Pd (B)

AFM images for all PVD films are similar regarding films topography. Typical AFM image for samples (2) and (3) are presented in Fig.4. On the surface of film we observed separated grains. AFM images are consisted with SEM images. The grain size studies for this was performed by the cross-section analysis tool.

For samples (2) average roughness (Ra - that is arithmetic average of the absolute values of the measured profile height deviation) was less then 20 nm while for sample (3) is less then 56 nm. Height of single nanograins was between 51-80 nm for sample (2) and between 190-230nm for sample (3). Grains in sample with higher concentration of palladium were higher than in sample with lower Pd content.

ACKNOWLEDGMENT

This research was co-financed by the European Regional Development Fund within the Innovative Economy Operational Programme 2007-2013 No UDA-POIG.01.03.01-14-071/08-00).

RAMAN STUDY

The samples were studied by means of Raman spectroscopy using Raman spectroscope Jobin Yvon-Spex T64000 triple monochromator equipped with a confocal microscope and CCD detector (with the resolution of 1024 x 256 pixels), cooled with liquid nitrogen. The studies were carried out using a single monochromatisation; Rayleigh dispersion was effectively prevented with Notch filters (for laser line 514.5 nm). Ar/Kr Laser (Laser-Tech, model LJ-800) was applied as an excitation source with $\lambda=514.5$ nm and 647.1 nm, power 50 mW. Acquisition of spectra was performed for spectral range 400 to 2000 cm⁻¹.

Raman spectra for samples obtained in PVD process are presented in Fig.5.

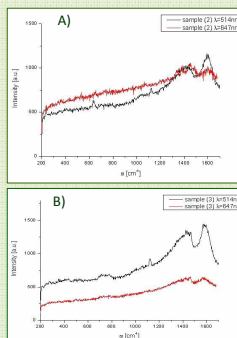


Fig.5. Raman spectra for samples: (2) A) and (3) sample B)

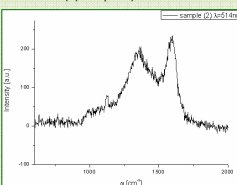


Fig. 6. Raman spectra for samples with different content of Pd and different conditions of excitation

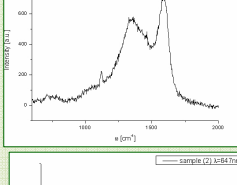


Fig. 6. Raman spectra for samples with different content of Pd and different conditions of excitation

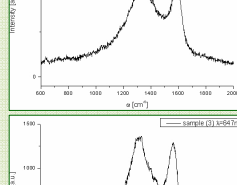


Fig. 6. Raman spectra for samples with different content of Pd and different conditions of excitation

Presented Raman spectra in Fig.5 obtained with excitation with beam $\lambda= 647$ nm have bands characteristic for fullerene C₆₀ molecule vibrations. Spectra obtained with $\lambda=514$ nm shows typical graphite-like bands (D- and G-band). From these Raman spectra we can deduced that laser beam with $\lambda= 514$ nm could activate fullerene degradation to graphite-like structure. The energy of this beam is higher than for beam with $\lambda = 647$ nm.

Raman spectra for listed above samples obtained in CVD process, having various Pd contents, are presented in Fig.6. Measured spectra were decomposed into bands using Lorentzian shape lines. This decomposition was carried out in Origin programme, which does not support the function of Voigt. The analysis showed existence of two main separated bands, placed at 1336 - 1361 cm⁻¹ (D-band) and at 1588 cm⁻¹ (G-band). To determine the level of graphitization, the intensity ratio ID/IG was found. Results of such analysis are presented in Table 2.

Table 2. Lorentz decomposition

Sample	D band		G band		I _D /I _G
	ω [cm ⁻¹]	FWHM	ω [cm ⁻¹]	FWHM	
Sample (2) ($\lambda=514$ nm)	1356.1	262.2	1589.7	73.2	1.218
Sample (2) ($\lambda=647$ nm)	1336.9	318.9	1587.5	79.2	1.306
Sample (3) ($\lambda=514$ nm)	1361.0	291.4	1585.8	74.7	1.125
Sample (3) ($\lambda=647$ nm)	1340.0	312.8	1587.1	81.0	1.308

Obtained spectra are a characteristic for graphite-like or amorphous carbon. The D -band is getting wider with increasing excitation energy, what is typical for all types of carbon [6-7]. However behaviour of the G-band is in opposite. The intensity ratio ID/IG provides information on a graphitization degree of the investigated structure. The graphitization degree of a material decreases with the increase of ID/IG value [2], therefore sample shown (2) less level of graphitization than sample (3).

CONCLUSIONS

1. Pd content increase affects on CVD process and then affects on final film form (composite grain size, porosity, Pd nanocrystals size and their dispersion)
2. Substrates form does not affect on the character of final film with some Pd content films remain porous
3. Porosity and ordering of porous carbonaceous matrix depend on the initial Pd content

REFERENCES

- [1] E. Terres, B. Panella, T. Hayashi, Y.A. Kim, M. Endo, J.M. Dominguez, Chem. Phys. Letter, vol. 403,(2005), pp.363-366
- [2] B. Panella, M. Hirsch, S. Roth, Carbon, vol. 43 (2005), pp. 2209-2214
- [3] J. Cabrila, M.J. Lopez, J.A. Alonso, Carbon, vol. 45, (2007), pp.2649-2658
- [4] Pavlovsky, P.Sundarrajan, Z.Yaniv, Sensors & Transducers Journal, Vol. 73, Issue 11, (2006), pp. 793-798.
- [5] E. Czerwos, E. Kowalska, H. Wronka, J. Radomska, patent modification, (2008) nr P384 91
- [6] Castiglioni, M., TommasiniOpt. Pura Appl, vol. 40 (2) 169-174 (2007)

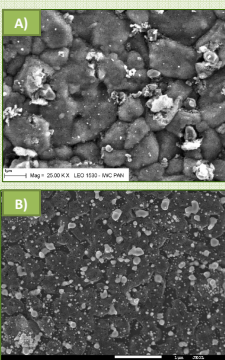


Fig.3 SEM images for samples 1 (A) and sample 3 (B)

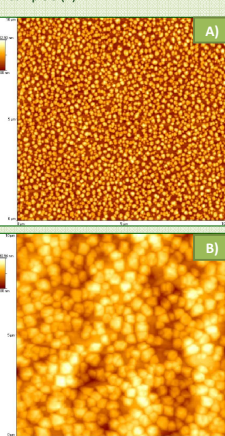


Fig. 4. AFM images for A) sample (2) and B) sample (3) (10x10 μm)